Proposal to Measure Hadron Scattering with a Gaseous High Pressure TPC for Neutrino Oscillation Measurements

C. Andreopoulos[25], G. Barker[30], S. Bolognesi[10], S. Bordoni[1], S. Boyd[30], D. Brailsford[13], S. Brice[3], G. Catanesi[8], Z. Chen-Wishart[16], P. Denner[30], P. Dunne[4], C. Giganti[12], D. Gonzalez Diaz[6], J. Haigh[30], P. Hamacher-Baumann[17], S.-P. Hallsjö[24], Y. Hayato[28], A. Ichikawa[11], I. Irastorza[33], B. Jamieson[31], P. Jonsson[4], A. Kaboth[16], A. Korzenev[22], Yu. Kudenko[9], M. Leyton[18], R.P. Litchfield[4], K.-B. Luk[20], W. Ma[4], K.B.M. Mahn[14], M. Martini[2], N. McCauley[25], P. Mermod[22], J. Monroe (P.I.)[16], U. Mosel[23], R. Nichol[21], J. Nieves[5], T. Nonnenmacher[4], J. Nowak[13], W. Parker[16], J.L. Raaf[3], J. Rademacker[19], T. Radermacher[17], E. Radicioni[8], E. Rondio[15], S. Roth[17], R. Saakyan[21], F. Sanchez[18], D. Sgalaberna[22], Y. Shitov[4], J. Sobczyk[32], F.J.P. Soler[24], A. Sztuc[4], C. Touramanis[25], Y. Uchida[4], S. Valder[30], J. Walding[16], M. Ward[16], M.O. Wascko[4], A. Weber[26], C.V.C. Wret[4], M. Yokoyama[27], A. Zalewska[7], M. Ziembicki[34], and M. Zito[10]

[1]CERN, European Organization for Nuclear Research, Switzerland
[2]ESNT, CEA, IRFU, Université de Paris-Saclay, France
[3]Fermi National Accelerator Laboratory, USA
[4]Imperial College London, UK
[5]Instituto de Fisica Corpuscular, Univ. Valencia - C.S.I.C, Spain
[6]IFGAE, University of Santiago de Compostela, Spain
[7]IFJ PAN, Krakow, Poland
[8]INFN Bari, Italy
[9]Institute for Nuclear Research (INR), Russia
[10]IRFU, CEA Saclay, France
[11]Kyoto University, Japan
[12]LPNHE, Paris, France
[13]Lancaster University, UK
[14]Michigan State University, USA
[15]NCBJ, Warsaw, Poland
[16]Royal Holloway, University of London, UK
[17]RWTH, Aachen, Germany
[18]Universitat Autonoma de Barcelona Institut de Fisica d'Altes Energies, Spain
[19]University of Bristol, UK
[20]University of California, Berkeley, USA
[21]University College London, UK
[22]University of Geneva, Switzerland
[23]University of Giessen, Germany
[24]University of Glasgow, UK
[25]University of Liverpool,UK
[26]University of Oxford, UK
[27]University of Tokyo, Japan
[28]University of Tokyo Institute for Cosmic Ray Research, Japan
[29]University of Warsaw, Poland
[30]University of Warwick, UK
[31]University of Winnipeg, Canada

CERN-SPSC-2017-030 / SPSC-P-355
25/09/2017

[32]University of Wroclaw, Poland
[33]University of Zaragoza, Spain
[34]Warsaw University of Technology, Poland

September 20, 2017

1 Executive Summary

We propose to perform new measurements of proton and pion scattering on Ar using a prototype High Pressure gas Time Projection Chamber (HPTPC) detector, and by doing so to develop the physics case for, and the technological readiness of, an HPTPC as a neutrino detector for accelerator neutrino oscillation searches. The motivation for this work is to improve knowledge of final state interactions, in order to ultimately achieve 1-2% systematic error on neutrino-nucleus scattering for oscillation measurements at 0.6 GeV and 2.5 GeV neutrino energy, as required for the Charge-Parity (CP) violation sensitivity projections by the Hyper-Kamiokande experiment (Hyper-K) and the Deep Underground Neutrino Experiment (DUNE). The final state interaction uncertainties in neutrino-nucleus interactions dominate cross-section systematic errors, currently 5–10% at these energies, and therefore R&D is needed to explore new approaches to achieve this substantial improvement. The proponents of this proposal are a consortium of detector development specialists and neutrino physicists collaborating on DUNE and Hyper-K. Many are authors of the Neutrino EOI submitted to the SPSC in early 2017 (SPSC-EOI-015); HPTPC development is a work package (WP9) within that framework.

Objectives

The motivation of this proposal is to develop the physics case, and begin conceptual design, for a neutrino detector that can achieve the unprecedentedly low neutrino-nucleus scattering systematic uncertainties needed for the search for CP violation in neutrinos. The specific objectives are to:

1. characterize the performance of an HPTPC prototype, with respect to track-finding, momentum threshold, angular and momentum resolution, proton vs. pion separation, and interaction multiplicity measurements;

2. measure proton-argon and pion-argon scattering cross-sections in the range of energies relevant for neutrino-nucleus interactions in DUNE and Hyper-K; and,

3. tune the NEUT and GENIE neutrino generators with new p-Ar data, and new π-Ar data, and then perform neutrino oscillation studies to assess the feasibility of achieving 2% systematic uncertainties.

Scientific Context

HPTPC detectors are an area of growing international interest. Both Hyper-K and DUNE have working groups on HPTPC detectors, the Tokai-to-Kamioka experiment (T2K) is exploring an HPTPC as a near detector upgrade, and European groups have held a series of workshops on HPTPC development over the last five years. In particular, two workshops in the past year hosted at CERN have featured HPTPC working group sessions. Given the recent indication of non-zero CP violation in the T2K data [1], it is timely to quantify the potential impact of HPTPC neutrino detector technology on mitigation of the dominant neutrino-interaction cross-section uncertainties for the future Long-BaseLine (LBL) programme.

HPTPCs will open a new window in neutrino scattering physics because this technique lowers the energy threshold for particle detection by an order of magnitude over current liquid argon and water Cherenkov detectors. This low energy region has the greatest sensitivity to resolve final state interaction model discrepancies, and therefore an HPTPC has unique capability to address the driving systematic uncertainty in neutrino cross-sections. At the end of this project the team will be in a position to quantitatively assess the physics potential of an HPTPC as a LBL neutrino oscillation near detector to achieve the neutrino interaction systematic uncertainty goals. This is highly relevant for both DUNE and Hyper-K: the Co-Invesigators on this proposal collaborate on both projects.

Beam Time Request

We request 28 days of beam time in 2018 in the East Area, preferably in T10 but also possibly in T9. We base this beam request on commissioning measurements of the low-momentum fluxes in T9 and T10 made in 2016, summarized in Section 3, implemented into a GEANT4 simulation of the HPTPC prototype detector, described in Section 4. The beam time request estimate is justified in Section 5.1.

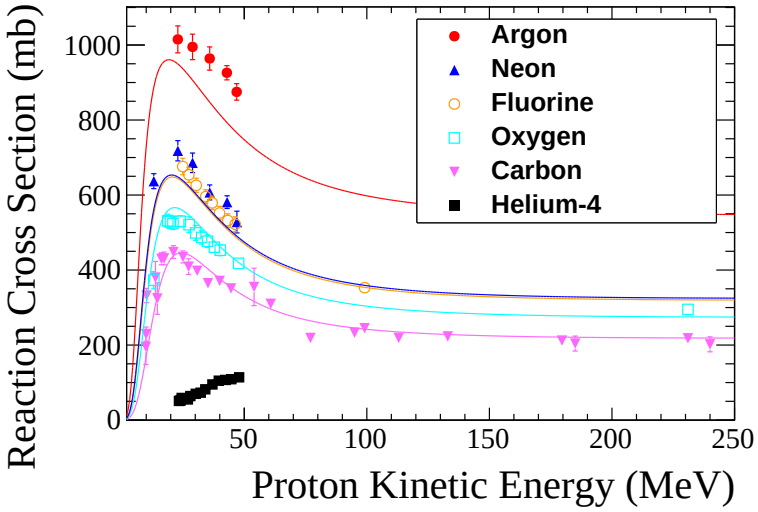

Figure 1: Total reaction cross-sections for protons on argon, neon, fluorine, oxygen, carbon, and helium-4. Data is shown against a semi-empirical model from Wellisch and Axen [2].

2 Context

The physics motivation for the R&D we propose is the search for CP violation and determination of the pattern of neutrino masses (mass hierarchy). These are among the most fundamental open questions in physics today.

2.1 Physics Motivation—The Search for CP Violation in Neutrinos

The major global effort in neutrino physics aims to understand why we live in a matter-dominated universe. CP symmetry violation in the neutrino sector is one of the few remaining possibilities to be explored experimentally. CP violation searches compare the rates of $\nu_\mu \to \nu_e$ and $\bar{\nu}_\mu \to \bar{\nu}_e$ oscillation, which, in the absence of CP violation, should be equal. To convert the measured rate of interactions to a level of CP violation, experiments must accurately know the cross-section for the interaction with the detector of both neutrinos and antineutrinos. Therefore, systematic uncertainties on cross-sections are a key input to such CP violation searches. These cross-sections are dependent on theoretical models because the target nucleon resides in a complicated nucleus, and the nuclear model has dramatic effects on the measured final-state particle kinematic distributions.

The current world's best accelerator neutrino oscillation experiment, T2K, reports neutrino interaction systematic uncertainties at the 5-7% level [3]. The future DUNE and Hyper-K projects assume systematic errors at the 1-2% level to achieve their physics goals, but will be in the same position as current experiments if the nuclear-model uncertainties are not reduced. The key to reducing these uncertainties is to measure precisely the multiplicity and momentum distribution of final-state particles [4]. These kinematic distributions are shaped by Final State Interactions (FSI) of the recoiling secondary particles as they leave the target nucleus. The most commonly used neutrino generator Monte Carlos, NEUT and GENIE, simulate FSI with cascade models that are tuned with external hadron-nucleus scattering measurements. However, as shown in Fig. 1, these proton-nucleus (and pion-nucleus) scattering measurements are extremely sparse and in many cases do not exist in the relevant momentum region and/or on the relevant nuclei. Therefore semi-empirical parameterisations are used to extrapolate in momentum and atomic mass. These parametrisations are different between NEUT and GENIE, and yield order-of-magnitude scale differences in the predicted multiplicity and kinematics of final state protons. The proton final state modeling is key for neutrino oscillation measurements because it affects the event selection and neutrino energy reconstruction. For these reasons, FSI effects represent a dominant contribution to the total neutrino interaction systematic uncertainty [3].

Gas TPCs are ideal for precisely characterizing FSI effects because of their high track recon-

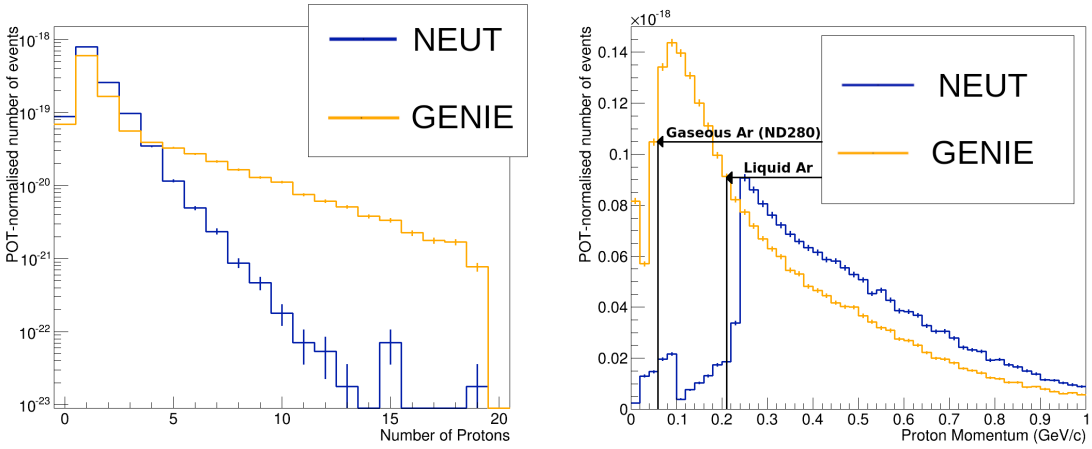

(a) Proton multiplicity.

(b) Momentum of protons exiting the nucleus.

Figure 2: Predictions from the NEUT (blue) and GENIE (orange) neutrino interaction generators of ν_μ CC interactions on argon in the T2K beam.

struction efficiency, low momentum threshold and 4π angular coverage of final state particles, which are all key to distinguishing between models. Fig. 2 shows the proton multiplicity and momentum distributions for ν_μ Charged Current (CC) interactions on argon calculated by the NEUT and GENIE neutrino generators. These distributions are highly discrepant, particularly in the fraction of events with few ejected protons, and at low proton momentum, below 250 MeV/c. This is below the proton detection threshold in water Cherenkov detectors (1100 MeV/c) and below that of liquid argon TPCs, around 400 MeV/c [5].

In the HPTPC we propose to prototype, the threshold for a well-reconstructed proton in argon at 5 (10) bar is 53 MeV/c (68 MeV/c) (Section 4.1), and therefore such a detector could probe the discrepant low-momentum region of parameter space in addition to covering the momentum range above 310 MeV/c (50 MeV kinetic energy) where no measurements exist (Fig. 1). This measurement range is highly complementary to what can be learned from the liquid argon ProtoDUNE beam tests.

2.2 Current State of Proton Scattering Measurements

The current state of proton-nucleus cross-sections is described in [6, 7], with data from protons in the range of 10 MeV–20 GeV on a broad range of nuclei interesting for neutrino interactions. The measurements on argon are shown in Fig. 1. The extant data comprise five points in the proton kinetic energy range of 23–47 MeV, with approximately 7% measurement uncertainty. These measurements were made using a thin gas target in a beam at the University of Manitoba [8]. The limited range of data available to constrain FSI models is a major contributor to the discrepancy between model predictions, shown in Fig. 2.

This lack of data is a promising opening for even a small prototype HPTPC to make competitive and useful measurements of proton-nucleus scattering in order to demonstrate the potential for HPTPC near detectors. We have built a prototype HPTPC, and propose to deploy it in T10 to measure the proton-Ar total scattering cross-section and, statistics permitting, differential cross-section in final state proton momentum. As discussed in Section 2.1, the small prototype we have built can populate a region with no existing measurements of protons on argon (between 50 MeV and 1 GeV). This is particularly interesting given the importance of argon to the future neutrino program and the significant disagreement between the argon data in Fig. 1 with models, discussed in [7].

To compare the available data to expected interactions, Fig. 3 shows the predicted kinetic energy of protons resulting from ν_μ CC interactions on argon, in a neutrino beam with peak energy of 0.6 GeV. The figure shows both the initial kinetic energy of protons which are generated inside the nucleus and the kinetic energy of those protons as they exit the nucleus; some of which have interacted in the nucleus on their way out. The interacting protons are predominantly below

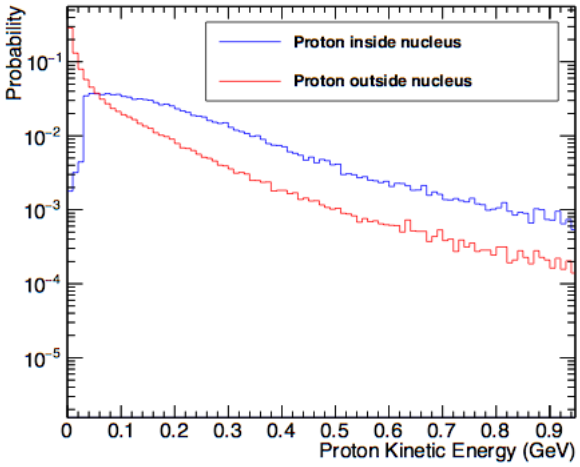

Figure 3: Predicted proton kinetic energy distributions from GENIE for 600 MeV ν_μ CC interactions on argon before (blue) and after (red) final state interactions (FSI).

0.2 GeV kinetic energy, but with a long tail that stretches beyond 1 GeV kinetic energy.

In the beam test with the prototype HPTPC, we propose to measure initial proton momenta between 0.2-1 GeV/c (or 0.02-0.4 GeV kinetic energy, sampling the peak of the blue curve in Fig. 3).

There is also a need for measurements on other nuclear targets. Fig. 1 shows the total reaction cross-section data on other elements, including helium, fluorine, and oxygen. There is only one measurement for each nucleus, over a limited energy range (above 20 MeV kinetic energy for protons, or 195 MeV/c). These nuclei are of interest as they are appropriate TPC gases for studying the A-scaling of neutrino interactions, used for e.g. extrapolating near detector measurements on argon to predict interaction rates on Oxygen in a far detector, as at T2K.

We propose to measure proton and pion cross-sections on argon in a 28 day run, and if time or parasitic running permit we would like to take an additional 2 weeks of data on Ne and CF_4, in order to span a range of targets from light (which is well studied, in particular for carbon) to relatively heavy (argon). We also choose these targets in order to have a calibration point relative to previous measurements. Given the readout electronics sampling rate and drift velocities, the prototype detector can measure final state particles in these target species by replacing the target gas, without changing the TPC internals or the readout.

As discussed in Section 2.1, the proton measurement is of primary importance however the pion data are also very interesting—the extant measurements for pion-nucleus scattering are similarly sparse as for protons [9], although the LARIAT experiment is currently making measurements with pions in this range. We propose a run plan tuned for measuring the proton cross-sections, but the pion measurement data will be collected simultaneously with the proton measurements.

3 Low Momentum Beam Flux in T9 and T10

To assess the feasibility of studying proton scattering in the range of interest for neutrino oscillation experiments (Fig. 3), measurements of the beam flux below 1 GeV/c were made in Summer 2016 on the T9 and T10 beamlines.

3.1 Time of Flight Measurement

The apparatus deployed to measure the flux is based on the Time Of Flight (TOF) system developed for the T2K experiment sub-detector commissioning runs in T9 in 2009. The system consists of two stations positioned at separated locations in the path of the beam. Fig. 4a shows the upstream TOF paddle in position in the T9 beamline. Each station has a small bar of fast scintillator,

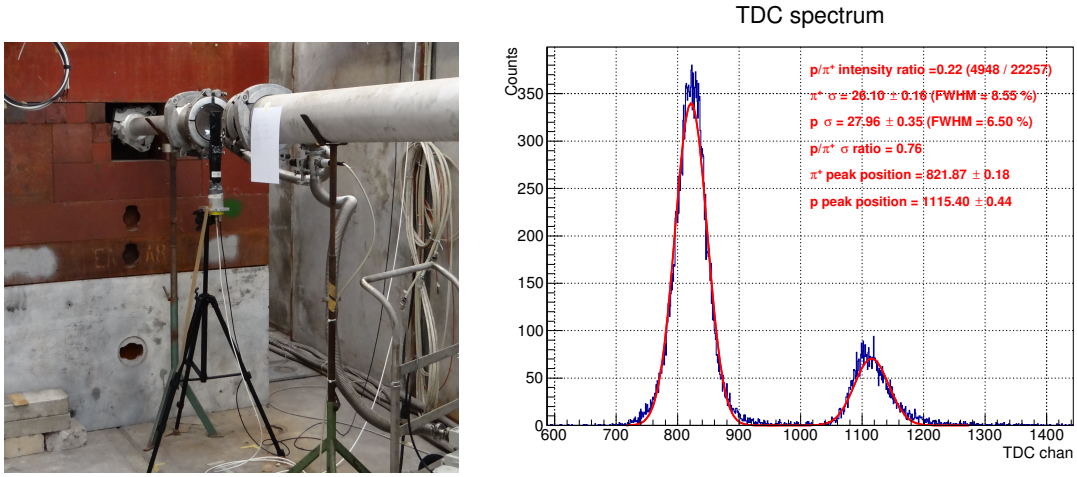

(a) Upstream TOF station in T9.

(b) Example of TOF spectra accumulated during a single run.

Figure 4: Components of the TOF measurement system, each station consisting of a cuboidal block of plastic scintillator coupled to PMT whose endcap is held in place with a tripod. Resulting TOF spectra in panel (b) show background-subtracted, fully separated peaks of pions/muons (left) and protons (right), fitted with Gaussian functions to estimate the yield in each peak.

connected to a fast PhotoMultiplier Tube (PMT) by a short light guide. A new DAQ system was developed to read out the PMTs, comprising a simple trigger/veto system implemented using NIM modules, a FAST ComTec 7072T TADC (used as a Time to Digital Converter), and a National Instruments PXIe unit running a LabView-based DAQ program and containing a Digital I/O module for communication with the TDC.

A raw measured TOF spectrum in the T10 beam is shown in Fig. 4b. Although the DAQ system was capable of sub-ns resolution, the system performance was limited by PMT timing to around 25 ns, which is still sufficient for proton and pion peaks to be well-separated at the momenta studied.

3.1.1 Analysis Procedure

Approximately 150 data runs were collected with an accumulated beam exposure of ∼30 hours. Run exposures varied between 240 and 3600 seconds depending on the experimental conditions, e.g. beam momentum, collimator setting, etc.

The raw data files contain the TOF digitized spectra. At beam momenta ≤ 1 GeV/c, the peaks of the protons and pions are completely separated. The intensities of the pion and proton particle peaks is calculated from the raw TDC spectra at the first stage of data processing. The peak intensity estimate is then refined after background subtraction; an example spectrum is shown in Fig. 4b. The background level was determined from the TOF spectrum outside the peak regions.

The intensity of protons varies from spill to spill. To measure this effect, beam set at 0.5 GeV with the standard collimator settings (14 mm $\times$ 14 mm) was designated as the reference run, and data were taken in this configuration before the start of each data run. The reference runs are used to calibrate for variations vs. time in the number of particles delivered per spill, shown in Fig. 5.

The intensity of protons also varies within each spill, and so we measure the deadtime of the TOF system DAQ as a function of time since start-of-spill. A 1-5% correction is applied for the time-dependent deadtime within each spill. We measured the deadtime vs. spill time at several points throughout the total data run and found minimal variation, and therefore one correction is derived and applied to all spills.

3.1.2 Results

The yield of protons and pions was measured in a set of runs with beam momenta in the [0.25,1.0] GeV/c range. The number of particles per spill for pions and protons, after spill intensity variation, background subtraction and deadtime corrections, are shown for T9 and T10 in Figs. 6 and Fig. 7 respectively.

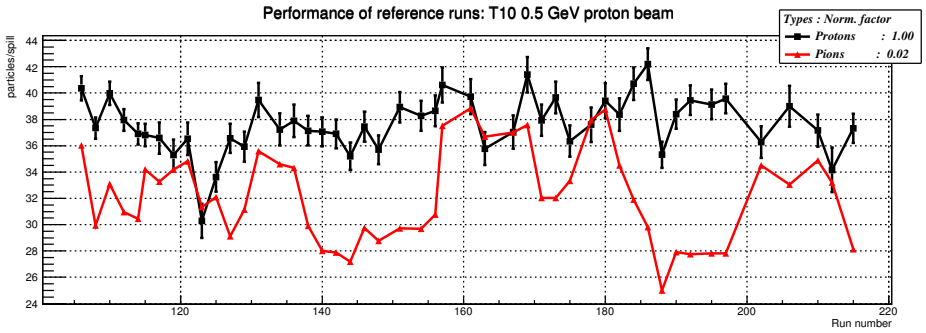

Figure 5: Variation of T10 beam spill intensity vs. run number, in reference runs during measurements spanning 30 hours.

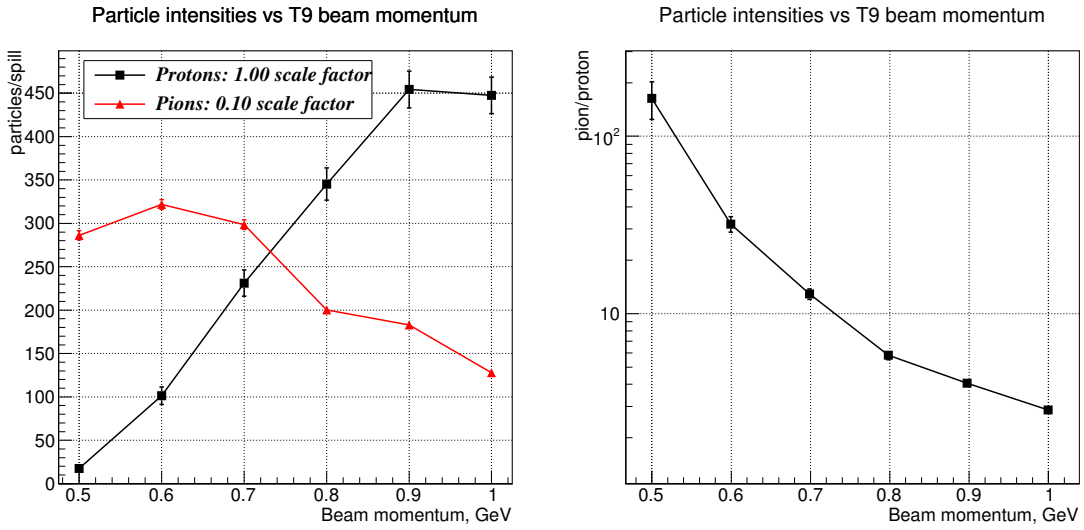

(a) (b)

Figure 6: Panel (a): Measured intensities of protons (black) and pions (red) delivered by T9 beam vs. proton momentum (GeV/c), in a low momentum ≤ 1 GeV/c range. The pions have been scaled by 0.1 for display. Panel (b): Measured ratio of pions to protons vs. proton momentum (GeV/c).

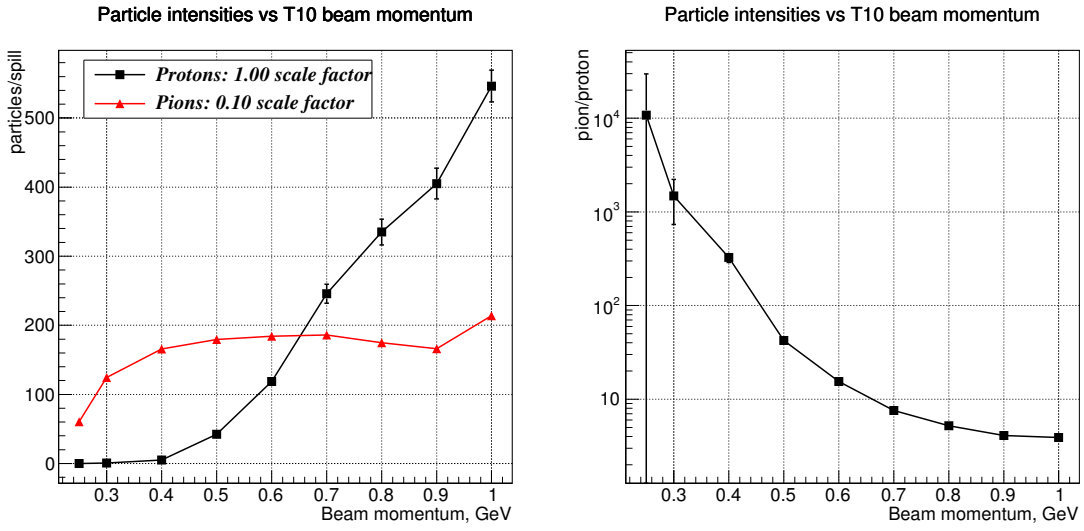

(a) (b)

Figure 7: Panel (a): Measured intensities of protons (black) and pions (red) delivered by T10 beam vs. proton momentum (GeV/c), in a low momentum ≤ 1 GeV/c range. The pions have been scaled by 0.1 for display. Panel (b): Measured ratio of pions to protons vs. proton momentum (GeV/c).

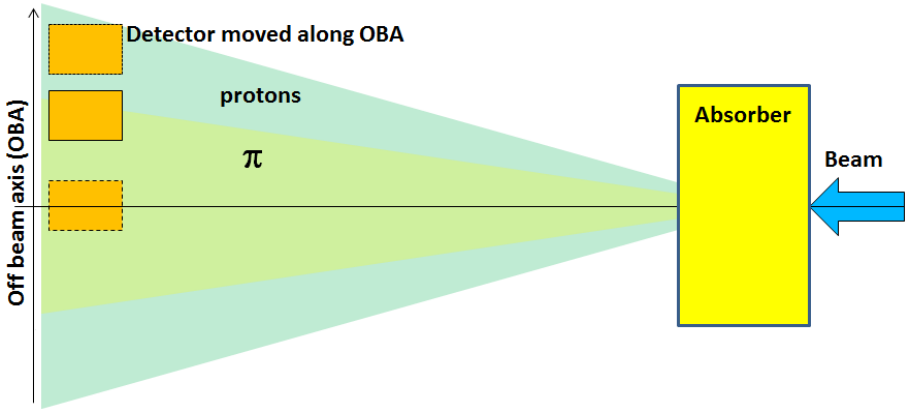

Figure 8: Schematic diagram of the off-axis measurement. The separation between absorber and line OBA is 13 meters.

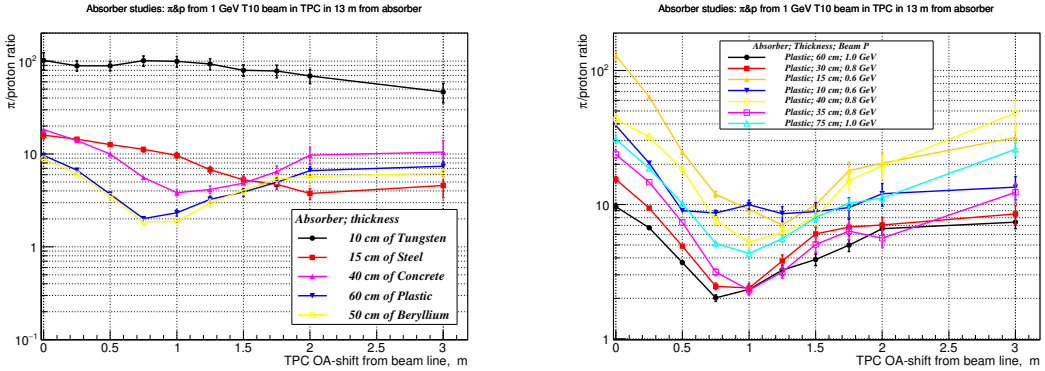

(a) Effect of using different moderator materials.

(b) Effect of beam momentum and moderator thickness.

Figure 9: The simulated π/proton ratio vs. off-axis angle, for various absorber materials and momenta in the T10 beam line.

In this configuration, there are few protons with momenta ≤ 0.5 GeV/c in T9 and ≤ 0.4 GeV/c in T10. To gain access to lower momentum protons, we developed an off-axis technique employing a moderator.

3.2 Off-Axis Measurement Technique

As protons are more likely to scatter at larger angles than pions in a moderator, placing the detector at an off-axis position with respect to the beam can offer a lower pion-to-proton ratio, as well as a lower momentum flux. This arrangement is shown schematically in Fig. 8.

To study this approach, data were taken in the T9 and T10 beamlines with concrete and steel absorbers. GEANT4 simulations of the beam passing through these materials were validated against the data and then used to optimise the absorber properties to produce a proton-enriched beam. The simulation models the prototype HPTPC dimensions, with a 0.5×1 m^2 area subtended by the TPC when viewed by the beam, located 13 m from a beam-pipe with dimensions of the T10 beam. The simulated number of particles entering the TPC, as a function of off-axis angle, particle type and absorber material are shown in Fig. 9a. As expected, absorbers made of light materials (e.g. plastic) produce lower pion-to-proton ratios.

The optimal absorber thickness and off-axis angle for measuring protons is estimated in Fig. 9b for various incident beam momenta. While the beam with larger initial momentum contains more protons, it requires a thicker moderator to minimize the pion-to-proton ratio, which results in greater spread of proton momenta after the absorber. The optimal configuration found is 0.6-0.8 GeV/c beam, with 35 cm of plastic absorber. At the optimum conditions, the simulation predicts an average flux of 7 protons and 15 π-related particles per spill into the active volume

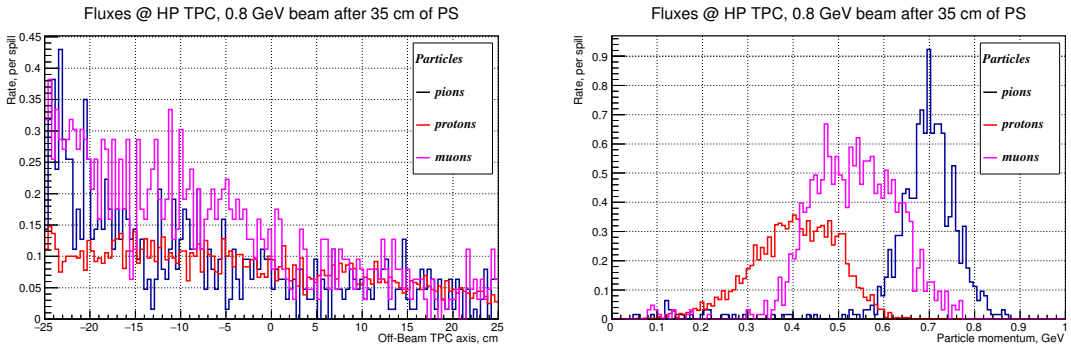

(a) (b)

Figure 10: Panel (a): simulated particle flux per spill vs. distance from beam center along off-beam axis. Panel (b): simulated particle flux per spill momentum (GeV/c). Distributions are shown for pions (black), protons (pink), and muons (red) impinging on the TPC in T10 with 0.8 GeV/c beam passing through 35 cm of plastic absorber. Spectra are normalized per beam spill.

of the TPC. The term π-related is used here because there is no π/μ separation in the deployed TOF system at these momenta. The spatial and momentum distributions of particles entering the detector in the optimum configuration are shown in Fig. 10.

4 High Pressure TPC Prototype

The detector we propose to deploy is a high pressure TPC prototype, currently being commissioned in London. Thus far, the TPC, readout, DAQ and control systems have been qualified in a relatively low pressure vessel, and the high pressure operations will commence in a custom-designed pressure vessel in late Sept. 2017.

4.1 Design Motivation

The key requirements which motivate the design of an HPTPC neutrino cross-section detector are:

1. sufficient target mass to achieve low statistical error on measured final state kinematic distributions;

2. low momentum threshold for final state particles, to resolve model discrepancies in order to reduce neutrino scattering cross-section uncertainties to the 1-2% level;

3. minimisation of readout costs where possible, given the relatively large readout area.

Requirement 1 can be fulfilled by adequately pressurising the gas target system. A $5 \times 2 \times 1$ m^3 Ar HPTPC near detector at 5 bar would yield 5.5×10^3 or 1.9×10^5 neutrino interactions when exposed to 10^{21} POT from the J-PARC (280 m, 0.6 GeV) or LBNF (459 m, 2.5 GeV) beamlines respectively.

Requirement 2 demands a high granularity readout system. For a 10 bar HPTPC with 0.5 m drift, the transverse diffusion-limited pitch is 500 μm. This pitch specification, and previous performance demonstrations from T2K [10] and DMTPC [11, 12, 13], suggest a minimum particle trajectory length of 5-10 mm for sound track reconstruction. This translates to a sub-10 MeV proton kinetic energy based on fits from Christophorou, Olthoff and Rao [14].

Requirement 3 can potentially be fulfilled by utilising optical TPC readout, which could maintain high readout granularity while costing 0.005 EUR/channel [15]. This readout approach has been demonstrated for dark matter applications by DMTPC at the 1 m^2 readout scale [16, 13].

4.2 Optical TPC Context

A relatively new development in TPC readout technology that offers a low cost per channel is optical readout. TPC technology has been in use since the late 1970s, typically with direct readout of

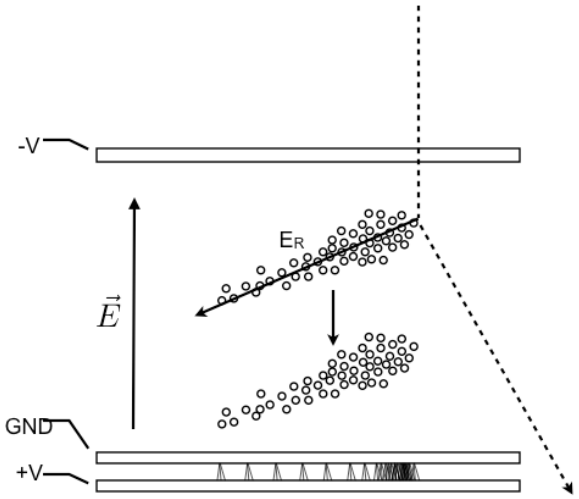

Figure 11: TPC schematic: a neutrino (dashed line) scatters a nuclear recoil that makes a track of ionisation; liberated electrons (open circles) drift to the amplification region where avalanches produce scintillation photons.

the drifted charge. 2D optical readout of time projection chambers was first demonstrated in 1994 and more recently has been developed by the DMTPC project for direction-sensitive dark matter searches, by the O-TPC experiment for precision nuclear physics cross section measurements, and by the CERN gas detectors group for gamma detection. For a recent review, we refer the reader to [17].

An optical TPC is instrumented with a cathode, ground, and anode electrodes which define its signal collection and amplification regions. Ionisation electrons from charged particles propagating through the TPC move in the drift field to the amplification region where avalanche charge multiplication and scintillation photon production occurs. In Ar gas with small (5%) admixture of CF_4, the scintillation photon yield in optical wavelengths is 0.1-0.3 per avalanche electron, and is a weak function of the reduced electric field. A schematic of how an optical TPC operates is shown in Fig. 11. The ground and anode electrodes can also be equipped with charge readout to provide high resolution tracking in the drift direction. A CCD or CMOS camera views the amplification plane through a lens from outside of the pressure vessel containing the TPC and target gas, collecting the scintillation light and subsequently providing tracking in the amplification plane. Each CCD pixel views an area of the amplification region which is larger than its pixel area, this optical plate scale is defined by the object and image distances and the camera lens properties. The area of the amplification plane which is viewed by a single physical pixel is called a *vixel* here, and the vixel size defines the detector's readout pitch.

4.3 Prototype Detector Specifications

The prototype HPTPC pressure vessel is a 5 bar, CE code-stamped pressure vessel built by Cryovac, measuring approximately 0.7 m length × 1.3 m diameter. A schematic of the TPC inside the pressure vessel is shown in Fig. 12a. The vessel during construction is shown in Fig. 12b. These dimensions indicate the approximate footprint of the pressure vessel needed for the beam test. The vessel is equipped with flanges for high voltage, gas and vacuum system connections, calibration, and optical and charge readout connections. The cylindrical section has ports for calibration and a specially constructed beam window flange with a small 2 mm thick Al window section.

The gas target handling system, shown schematically in Fig. 12a, is monitored by a Slow Control (SC) computer via a pressure transducer. The SC controls bottle-to-vessel and pump-to-vessel solenoid valves for pressure control. The SC system fills the pressure vessel from a gas bottle via a mass flow controller up to 5 bar pressure. Prior to filling, the chamber can be evacuated to 0.01 bar by a connected scroll pump in order to achieve required gas purity levels. There are two independent, redundant relief lines, each with a 5 bar burst disk.

We have built a prototype TPC with dimensions chosen to test the key track reconstruction

parameters needed for a full size (10 m^3) neutrino detector: diffusion over 0.5 m drift length, and pitch over a m^2 readout area. The TPC design, prototype HPTPC readout, and data acquisition software are based on that demonstrated by the DMTPC experiment with several members of the proposal team (J. Monroe and A. Kaboth) bringing significant prior DMTPC experience.

The prototype TPC is shown in Fig. 13, it is currently being commissioned with a 50% length field cage in a vessel capable of 1 bar pressure, at RHUL. The drift length of the full field cage is 0.6 m, and the diameter of the field cage is 1.2 m. The TPC is mounted to rails welded onto the cylinder body. The cathode, ground, and anode electrodes are constructed of 250 μm pitch stainless steel mesh [18] tensioned to 25 N-m, and epoxied to stainless steel supports. The ground and anode electrodes are separated by 1 mm by resistive spacers, and mounted on delrin rods that form the support assembly. The stand-off distances for the supports are chosen such that the anode electrode can operate up to 1 kV, and the cathode electrode up to 7.5 kV. The cathode voltage requirement is to define a 150 V/cm drift field, in order to miminize diffusion in the drift region. The field cage ring spacing was simulated in COMSOL, and chosen to be 3 cm in order to achieve 1% drift field non-uniformity in the fiducial region. Given this spacing, the drift region is enclosed by 18 Cu field cage rings.

There are two optical readout options available to use with the TPC, one with 500 μm pitch employing one camera to image the entire amplification plane, and the other using four cameras, achieving 250 μm pitch. Both cameras may be operated in a readout mode where pixels are summed in hardware prior to readout, allowing for 2×2 up to 8×8 spatial binning in order to test larger pitches.

The baseline optical readout uses four FLI Proline PL09000 CCDs centered on each quadrant of the amplification plane. The FLI Proline PL09000 has 3056 × 3056 12 μm × 12 μm pixels with 10 e^- read noise coupled to Nikon f/1.2 50mm focal length lenses with a 54.8° angle of view. At an object distance of 85 cm the system images a 71×71 cm field of view with a vixel size of 230 μm. An image showing 25 MeV/c alpha particles in the TPC recorded during commissioning with this camera system in Sept. 2017 is shown in Fig. 13. The estimated signal-to-noise for 50 MeV/c tracks in this optical system is 6-8.

The Spectral Instruments 1100s Fairchild CCD has 4096 × 4112 15 μm × 15 μm pixels with 5 e^- readout noise. This camera is large enough to image the entire amplification region when coupled to a Canon f/0.95 50mm focal length lens, with a 86° angle of view. At an object distance of 85 cm the system images a 120×120 cm field of view with a vixel size of 500 μm. The estimated signal-to-noise for 50 MeV/c tracks in this optical system is 10-12.

The charge readout uses CAEN N6730 500 MHz digitizers to record the anode and mesh electrode signals. These are segmented into four quadrants spatially, in order to lower the capacitance. The anode signals are amplified by CREMAT CR-113 charge-sensitive pre-amplifiers, the ground plane (mesh) signals are amplified by CAEN A1423 Wideband amplifiers. The typical noise of the charge readout is <0.5 mV per time sample, allowing sensitivity to tracks depositing as little as 5.9 keV in the TPC drift region.

The charge and optical signals are associated in the data acquisition software, in order to combine the amplification plane readout samples (from the CCD) with the drift direction samples (from the charge readout). This hybrid readout system was designed for low-multiplicity dark

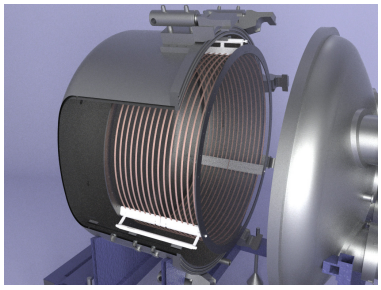

(a) Cut through view of the HPTPC Vessel with TPC shown.

(b) Prototype high pressure detector vessel

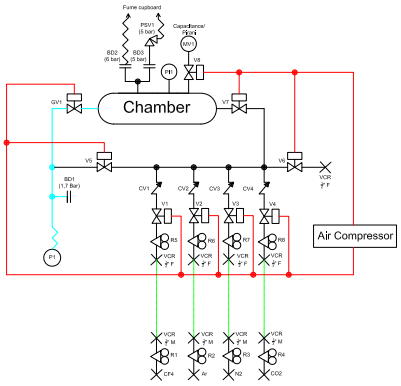

(c) Schematic view of the gas system.

Figure 12: Overview of HPTPC components.

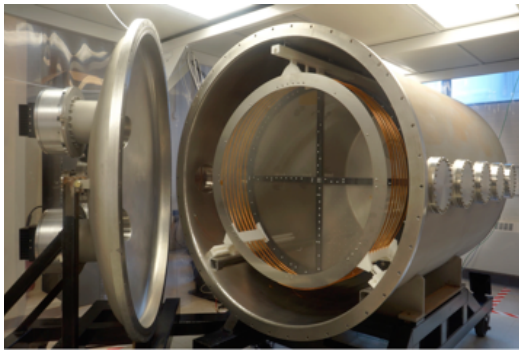

(a) Photograph of the HPTPC TPC, showing cathode, field cage rings and amplification region.

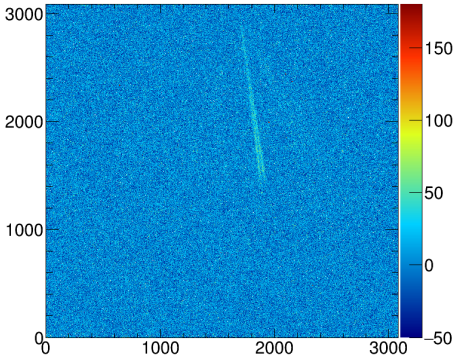

(b) CCD data event display from TPC commissioning in a low pressure test stand vessel.

Figure 13: Commissioning data from the HPTPC TPC, installed in a low-pressure test stand. The event display in panel (b) shows a CCD image of 25 MeV/c alpha particles, during commissioning of the TPC shown in panel (a) with ProLine09000 CCD. The color scale indicates the detected photon intensity per pixel, after bias subtraction, vs. pixel number along the X and Y readout axes.

matter applications, however it is sufficient given the relatively low occupancy of the beam test.

The HPTPC will be deployed with the TOF system used to study the low-momentum beam flux, and augmented with a larger, segmented TOF system being developed in Geneva and UCL. This will allow the initial momentum determination from the moderated beam and assist in position reconstruction in the HPTPC.

4.4 HPTPC Prototype Simulation and Reconstruction

In order to estimate the efficiency of the HPTPC prototype in identifying proton interactions, we simulate the measured T10 flux with the noise performance parameters measured in the prototype. These simulated interactions are then passed to the reconstruction software.

4.4.1 Simulation Software

The simulation of the HPTPC is based on existing C++-software using GEANT4 developed for the DMTPC experiment [11], which has been extensively verified against DMTPC data. In the simulation, energy deposition through the gas is modelled by the SRIM package [19]. The response of the detector is modelled by GARFIELD++ [20] in the drift and amplification regions, and the readout response is parameterized using the measured noise. The energy and direction of simulated particles are drawn from the T10 beamline geometry indicated in Fig. 8. A parameterised response model allows the simulation to run very quickly to test different hardware configurations.

Protons and pions are simulated individually in the Monte Carlo simulation and the tracks produced are saved in an ntuple. The probability, P(TPC), of a proton or pion (or one of their daughter particles) entering the TPC active region is estimated from the Monte Carlo simulation. To ensure realistic pileup in the simulated CCD images, the multiplicity (N_{Tracks}) is modelled as a Poisson distribution with mean, N, given by $\mathrm{N} = N_{\mathrm{spill}} \times \mathrm{P(TPC)}$ and N_{spill} is the number of particles per spill. N_{spill} has been measured for the T9 & T10 test beams at a range of momenta detailed in Section 3. Individual tracks are then merged together according to the calculated multiplicity to produce the simulated CCD images. Fig. 14a and Fig. 14b show respectively a typical off-axis and on-axis simulated CCD image.

4.4.2 Reconstruction Software

The track reconstruction software uses the T2K TPC Reconstruction EXtension (TREx) software developed by Warwick and Imperial College [21]. TREx produces a hierarchy of objects: patterns, paths and junctions:

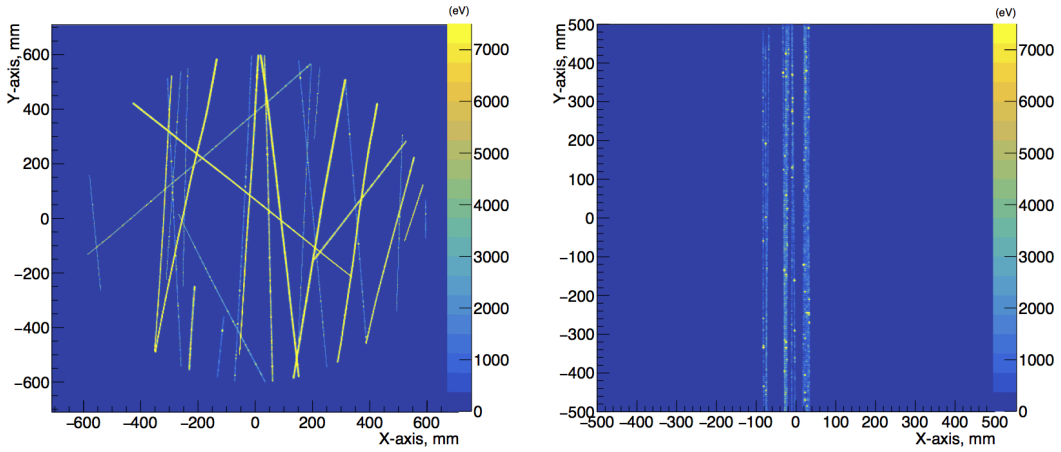

(a) Typical simulated CCD output of an off-axis spill: 0.8 GeV/c inital beam, Prototype HPTPC 3°- 4° off-axis and 13 m downstream of a 30 cm thick plastic moderator.

(b) Typical simulated CCD output of an on-axis spill: 0.3 GeV/c beam aligned with 2 mm thick aluminum beam window.

Figure 14: Simulated CCD event displays. The color scale indicates the detected photon intensity per pixel, without bias subtraction, vs. pixel position along the X and Y readout axes (mm).

1. *Patterns* are formed of any contiguous group of CCD hits connected together by the pathfinding. Patterns can contain an arbitrary combination of paths and junctions.
2. *Paths* are routes between points of interest. A single particle trajectory will ideally create only a single path, but may break into multiple paths if it passes any points of interest before leaving the TPC (e.g. delta ray production). In addition to belonging to the pattern, hits along a path belong to that path.
3. *Junctions* are points at which two or more paths meet. Junctions can also be formed by e.g. hadronic interactions, such as the signal interactions in the CERN test beam data.

TREx uses the A* algorithm [22] to find paths between given points of interest. The path is built up by stepping through discrete points in space (in this case, the CCD pixels), selecting the point that has the lowest cost. The cost at each step comprises two terms: the connection cost, representing the sum of point-to-point connections made to reach the current position, and the heuristic cost, representing the estimated cost of reaching the end point from the current position.

TREx identifies the points to be connected using a multi-stage approach:

1. *First Pass Edge Detection*: All CCD pixels at maxima and minima in Y or Z are selected to identify the points of interest at which particles enter or leave the detector.
2. *Junction Detection*: If three or more points of interest emerge from the first two stages, the pathfinding now searches for junctions where these paths meet. These are identified by using A* to navigate between the edge points, and finding the position at which the paths begin to diverge.
3. *Kink-Finding*: Vertices with only two outgoing particles will not yet have been found by the edge or junction detection. To identify these, the pathfinding looks for sharp kinks in the path. This concludes the pattern recognition.
4. *Tracking*: A straight track fitting algorithm is used to further reconstruct a particle track from the clustered path hits. This allows the extrapolation of track states in order to match and merge across junctions, using a likelihood method. Though originally developed to recover continuous tracks from paths that are broken due to δ-ray emission, this turns out to play an important role in solving ambiguities that arise from the 2D nature of the amplification plane readout. We have not yet fully merged the charge readout information into the reconstruction algorithm.

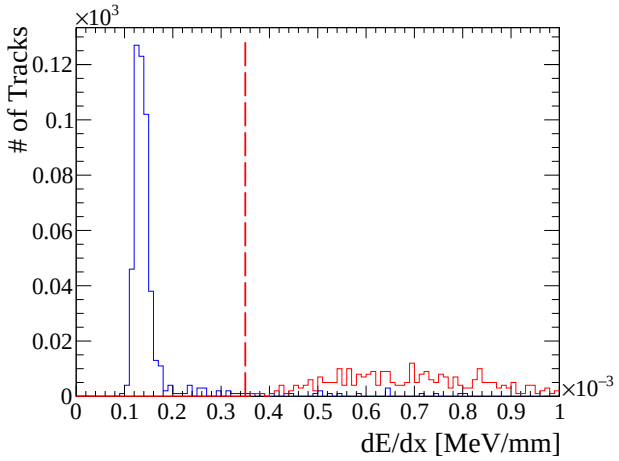

Figure 15: Simulated energy deposition in the detector for single track pions and muons (blue) and protons (red). A dE/dx cut at a value of 0.35×10^{-3} MeV/mm provides a good veto of the characteristic MIP peak.

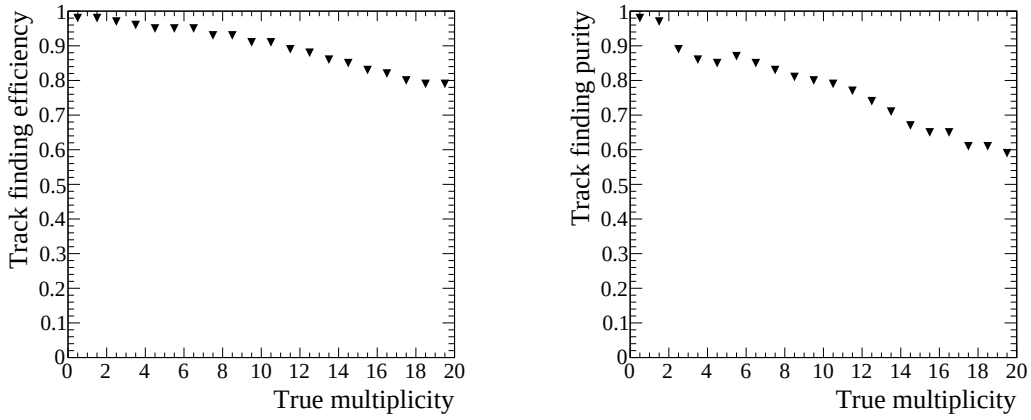

Figure 16: Simulated track reconstruction efficiency (left) and purity (right), for tracks passing a hit completeness requirement of 50%, as a function of the true number of tracks in the event.

5. *Particle Identification*: A simple PID algorithm based on a dE/dx cut is applied to distinguish protons from pions and muons. A study of simulated single tracks of known particle type ascertained that a cut value of 0.35×10^{-3} MeV/mm can provide clear discrimination of particle types as can be seen in Fig. 15.

An overall proton reconstruction efficiency is determined from the two underlying efficiencies: a basic track finding efficiency and a PID efficiency as $\epsilon_{\text{tot}} = \epsilon_{\text{track-finding}} * \epsilon_{\text{pid}}$.

We expect the performance of the track reconstruction to be dependent on the signal-to-noise and on the track multiplicity in the prototype HPTPC. Optimizing the quencher gas fraction and reduced electric field for operation can increase multiplication and the photon-to-electron yield to maximize signal-to-noise; collaborators in Spain and Germany have expertise to simulate and test stands to measure optimal mixtures at high pressure. We examine here how the performance is affected by increasing track multiplicities from 1 to 20 using the MC. We define a basic track efficiency and track purity, shown in Fig. 16, imposing the minimal condition that at least 50% of true vixel hits have been clustered correctly. We see an overall good track reconstruction performance that does, however, degrade at high multiplicities due to the aforementioned ambiguities. For this reason we intend to operate with collimator settings that limit the number of tracks going into the TPC active volume to ∼20 per spill. We measured that a reduction of up to a factor of 7 is

feasible by reducing the horizontal and vertical collimator apertures in both the T9 ad T10 beams, relative to the reference run settings used in acquiring the low-momentum flux data reported in Section 3.

Once a track has been reconstructed, the associated charge can be used to determine an average dE/dx. We then apply the pion and muon veto based on our study of single tracks, shown in Fig. 15. Events that pass the veto are assumed to be a proton. The proton PID efficiency and purity are summarised in Fig. 17, which shows this is a reliable method of identifying true protons.

5 Beam Test Measurement Plan

The goal of the test beam run we propose is to study the response of the hybrid optical-charge HPTPC to known particle species with momenta similar to those produced by interactions of neutrinos with energies of a few GeV, as would be expected from the T2K, Hyper-K or DUNE experiments. Moreover, we have identified a need for new measurements of proton-argon scattering for use in tuning neutrino interaction generators. We justify the requested beam test duration by estimating the proton-argon scattering event rates, including the simulated effects of track-finding and proton identification efficiencies.

5.1 Data Collection and Measurement Plan

After shipping the detector to CERN, we project that 14 days will be required for installation, integration of the trigger system into the DAQ and system integrity checks. This can all be done off-beam or in a parasitic mode. Following this, we request 28 days of beam time to acquire data at a range of beam momenta on Ar target gas. If additional time is possible, we would like to extend the run by 2 weeks to study scattering on CF_4 and Ne. This time does not need to be contiguous with the primary 28 days.

The baseline run plan we request is to acquire sufficient statistics to make a competitive measurement in the limited range of the Carlson Ar data shown in Fig. 1, and extend to both higher and lower momenta. The extant data have 7% total errors, with statistical error and fiducial mass error dominating that number [8]; to make competitive measurements we aim to achieve statistical errors of 3–5% in multiple bins of proton kinetic energy, so we have targeted 5,000 identified proton-Ar interactions.

To estimate the beam run duration, we calculate interaction rates using a Monte Carlo study based on the T9/T10 beam flux measurements and our GEANT4 detector simulation. At 0.8 GeV/c momentum setting (with collimators set at 14 mm × 14 mm), we expect 335 protons/spill. In our

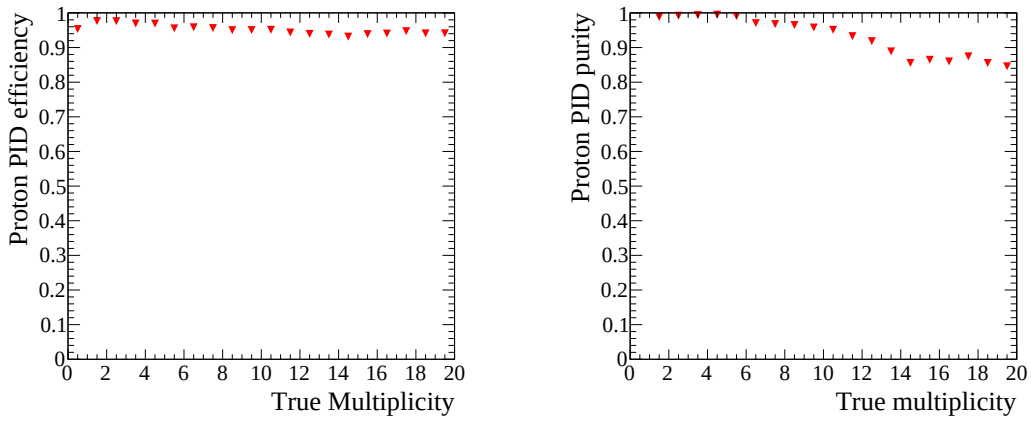

Figure 17: Simulated proton PID efficiency (left) and purity (right) vs. true number of tracks in an event, after pion/muon veto cut. The efficiency is mostly flat with multiplicity, indicating that true protons are rarely not identified whereas the slight dip in purity is due to pion tracks with embedded proton hits that are therefore reconstructed with a higher-than-true charge.

Configuration	P (GeV/c)	Moderater	Spills	Duration (days)
On-axis	1.0	None	5,000	1
On-axis	0.3	None	5,000	1
Off-axis	0.8	Plastic	80,000	26

Table 1: Baseline beam data run plan for CERN PS East Area Test Beam. The primary physics run is in the off-axis configuration, collecting enough spills for at least 5,000 cleanly reconstructed proton signal interactions. The duration estimate at each momentum assumes 1 cycle per PS supercycle, and 50% duty factor.

off-axis position, ∼2% of those protons reach the TPC active volume, yielding approximately 7 protons and 15 pions/muons per spill. The cumulative proton reconstruction efficiency from simulation is 70%, this is estimated as the product of 75% track reconstruction efficiency for a multiplicity of 20 tracks (Fig. 16) and 95% proton PID efficiency (from Fig. 17). With interaction cross-sections ranging from 500 to 1500 mb, the interaction probability is 0.5% to 1.5% in the TPC fiducial volume at 5 bar pressure of Ar. Thus, we estimate that 80,000 spills are needed to identify and reconstruct 5,000 p-Ar interactions.

Given the PS 14 second super-cycle, and assuming 50% duty factor, 26 days of dedicated running are required in off-axis configuration. The 50% duty factor is estimated as the product of 80% beam uptime, 80% detector uptime (to account for gas refills required to preserve gain stability), and 80% physics uptime (where the remainder is for calibration, reference runs, etc.) We will start with two days of instrumental calibration runs on-axis, at 1 GeV/c and 300 MeV/c for calibration of the TOF and detector PID. This request is outlined in Table 1.

5.2 Test Beam Data Analysis

The cross-section measurement method is based on the sliced TPC approach developed by the LAr TPC In A Test-beam experiment (LArIAT) [23]. The TPC active volume is treated as a series of thin Ar slabs which are perpendicular to the beam direction. In the case of our HPTPC prototype, the CCD vixel columns define the minimum thickness of the Ar slabs. With such a treatment, the cross-section, σ, as a function of kinetic energy, E, can be approximated as

$$\sigma(E) \approx \frac{1}{z n_{\mathrm{Ar}}} \frac{N_{\mathrm{I}}(E)}{N_{\mathrm{In}}(E)}, \tag{1}$$

where n_{Ar} is the number density of each Argon Slab (ArS), z is the depth of each ArS, N_{In} is the number of particles incident on each ArS and $N_{\mathrm{I}}(E)$ is the number of particles interacting in each ArS.

The full analysis will use TREx patterns as inputs but as a proof of concept of the method, the GEANT4 simulation described in section 4.4 has been used with a simplified model of the CCD and its readout for protons only, without the full diffusion, recombination, or impurity effects. The kinetic energy of a proton as it passes the nth vixel column is

$$E = E^0 - \sum_{i=0}^{n} E_i, \tag{2}$$

where E^0 is the energy of the proton as it enters the TPC active volume and E_i is the energy deposit measured by the ith vixel column. E^0 is assumed to be known with perfect precision and accuracy in this proof of concept analysis. For each slab, the proton is recorded in a distribution binned in kinetic energy where each bin represents $N_{\mathrm{In}}(E)$. This process repeats until the proton undergoes an elastic or inelastic scatter (assuming 100% identification efficiency) or exits the TPC active region. An example of an identified scatter is shown in Fig. 18a. For each slab, every identified scatter is recorded in a kinetic energy distribution, where the bin contents represent $N_{\mathrm{I}}(E)$. The bin-by-bin ratios of the two distributions are used in equation 1 to calculate the scattering cross-section binned in kinetic energy, which is shown in Fig. 18b. The statistical errors shown here correspond to the beam test request, and are competitive with the extant measurements in the limited range where these exist. To reduce statistical uncertainties we can of course choose a coarser binning for the differential measurement.

The final analysis will utilise the TOF in the estimation of E^0, but must include an estimate

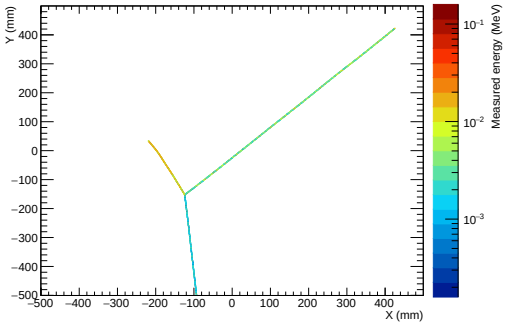

(a) An image of a proton undergoing an inelastic scatter as observed from the simplified simulation of the CCD. Each bin represents a vixel. The incoming proton enters from the bottom of the image.

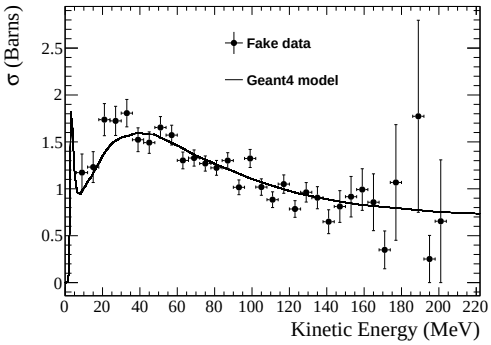

(b) The proton scattering cross-section measured using the sliced TPC method on fake data (black points) and compared with the input GEANT4 cross-section model (black line). The error bars are statistical only.

Figure 18: The sliced TPC analysis of the simulation described in section 4.4 with a simplified simulation of the CCD readout. The complementarity of the proposed measurements can be seen by comparing the measurement sensitivity estimate in panel (b) with the extant data in Fig. 1.

of the energy loss in the vessel wall, which we expect to be the largest systematic uncertainty in the measurement.

6 Resources

6.1 Request from CERN

We request:

1. 28 contiguous days of beam time with an additional 14 days if time is available, in the T9 or T10 beam line.
2. Sufficient space in T9 or T10, 13 m downstream of the beam-pipe end, to house the pressure vessel, gas system and electronics rack footprint for the entire run period. We estimate this is a maximum of 2.5 m $\times$ 2.5 m. If T10 space clearance is not possible, then we request an equivalent space in T9. It will not be feasible to split the run between T9 and T10.
3. 2 weeks of space out of the beam, or in a parasitic mode, for commissioning. Once the detector is shipped and reassembled at CERN, we will commission *in situ* using weak radioactive sources. Here the purpose is not to fully characterise the detector performance, but simply to confirm that all of the amplification region is live and that we observe the same system gain as in the laboratory commissioning.
4. Use of a clean tent (class 7) for the day of the TPC insertion.
5. Use of Ar, N_2 and CF_4 gas (research grade) for commissioning and operation of the detector at CERN.

6.2 Other Funding

The prototype HPTPC construction is funded by a UK STFC Project Research & Development grant, and the STFC Long Baseline Neutrino Strategy grant. Time of flight system contributions are planned from Geneva and UCL, gas optimization measurements from Aachen, Barcelona and Compostela, simulations effort is contributed by Spain and the UK, reconstruction and analysis efforts by Glasgow, Warwick, Lancaster, Germany, and the USA groups. CERN neutrino test beam effort is planned from the Canada, Germany, Italy, Russia, Spain, Switzerland, UK, and USA groups. Neutrino cross section model building and neutrino generator tuning work is the contribution of Saclay, Valencia, Giessen, ICRR, Wroclaw and Liverpool.

6.3 Track Record of Proponents

We highlight here the track records of the UK Co-Investigators involved in the prototype HPTPC construction grant in the UK: Wascko currently serves as the International Co-Spokesperson of the T2K experiment. Kaboth is the DUNE Near Detector Coordination Manager and T2K convener of the Beam and Near Detector Flux Fitting Working Group, and has extensive experience of optical TPCs. Nowak is the physics coordinator for ProtoDUNE-SP at CERN and an author of the neutrino interaction generator NuWro. Barker is a leading authority on track reconstruction in liquid argon detectors. Boyd has been involved in the measurement of neutrino interaction cross-sections and neutrino oscillation experiments for two decades; in the course of this work he has been involved in two, and led one, testbeam effort at the CERN East Area in the context of testing near detector prototypes for various neutrino experiments. Walding has deep expertise on neutrino cross-section measurement from the SciBooNE and MINERνA experiments. Monroe has made many of the measurements establishing optical readout as a viable technique in direct dark matter searches as leader of the DMTPC project, and serves on the Fermilab Long Baseline Neutrino Committee and the CERN SPS and PS Experiments Committee.

Since the UK funding (starting in 2015), the HPTPC development work has grown to engage the European community more broadly, with a series of workshops and joint DUNE-Hyper-K working group meetings. The proponents of this research are strongly engaged in the international neutrino programme, which has been identified as one of the highest science priorities in Europe. This HPTPC development project is embedded within the Expression of Interest for TPC-Based Near Detectors for Neutrino Long Baseline Experiments submitted to CERN in 2017 from 191 authors at 38 institutes in 12 countries (SPSC-EOI-015, work package 9).

7 Conclusions

For reducing neutrino oscillation systematic uncertainties in future experiments, a key measurement is proton-nucleus scattering. This process obfuscates the secondary particle multiplicity and kinematics, causing event migrations between data samples and introducing biases in neutrino event reconstruction. We propose to collect sufficient statistics in the HPTPC beam test for 3–5% statistical uncertainty on a proton-nucleus scattering cross-section measurement in binned in kinetic energy. Utilising the test beam's pion component, we can also potentially measure pion scattering processes including charge exchange and absorption, leveraging the expertise of LARIAT collaborators, particularly the Fermilab group on this proposal.

Once complete, we aim to use the p-Ar cross-section measurements to tune the NEUT and GENIE neutrino interaction generator MC FSI simulations, both of which draw interaction probabilities at each particle step from models fit to hadronic scattering data, highlighting the criticality of the broad measurement programme discussed in section 2.2. The authors of these generators are collaborators on this proposal. The tuned generators will then be used in full end-to-end neutrino oscillation sensitivity studies. The goal is to use the full range of interaction models available, and demonstrate quantitatively what gain in sensitivity can be achieved with the improved phase space acceptance of a gas HPTPC detector. Developing the framework for this work is underway by T2K and DUNE collaborators on this proposal.

We highlight that one of the lessons learned by recent attempts to use neutrino interaction measurements in global fits to extract neutrino model parameters is the importance of having full covariance matrices between data sets [24, 25]. Thus the data we propose to collect potentially allow a unique improvement over past measurements with correlations between p-Ar and π-Ar measurements. We also aim eventually to analyze this data coherently with the higher-momentum ProtoDUNE-SP measurements and lower-momentum LARIAT measurements, interfacing through Nowak, Brailsford and Raaf.

The measurements proposed here provide underpinning capability for future scientific projects in LBL neutrino oscillation experiments. This work will produce new measurements, useful in their own right, and provide 'neutrino engineering' input needed for the step-change precision required in neutrino cross sections for the DUNE and Hyper-K sensitivity goals. After the completion of the proposed work, we will be in a position to design a realistic-scale HPTPC neutrino near detector since we will have a reliable path from hardware specifications to full-size detector performance, benchmarked against these data.

References

[1] M. H. for the T2K Collaboration, T2k neutrino oscillation results with data up to 2017 summer, https://www.t2k.org/docs/talk/282, 2017.

[2] H. Wellisch and D. Axen, Physical Review C **54**, 1329 (1996).

[3] T2K, K. Abe *et al.*, Phys. Rev. Lett. **118**, 151801 (2017), 1701.00432.

[4] L. Alvarez-Ruso *et al.*, (2017), 1706.03621.

[5] MicroBooNE-Collaboration, MICROBOONE PUBLIC NOTE **1024** (2017).

[6] R. Carlson, Atomic Data and Nuclear Data Tables **63**, 93 (1996).

[7] H. P. Wellisch and D. Axen, Phys. Rev. C **54**, 1329 (1996).

[8] R. F. Carlson *et al.*, Nuclear Physics A **445**, 57 (1985).

[9] LADS Collaboration, D. Rowntree *et al.*, Phys. Rev. C **60**, 054610 (1999).

[10] T2K ND280 TPC, N. Abgrall *et al.*, Nucl. Instrum. Meth. **A637**, 25 (2011), 1012.0865.

[11] S. Ahlen *et al.*, Physics Letters B **695**, 124 (2011).

[12] C. Deaconu, Recent updates from the dark matter time projection chamber (dmtpc) collaboration, TAUP, 2013.

[13] C. Deaconu *et al.*, Phys. Rev. **D95**, 122002 (2017), 1705.05965.

[14] L. G. Christophorou, J. K. Olthoff, and M. V. V. S. Rao, Journal of Physical and Chemical Reference Data **25**, 1341 (1996), http://dx.doi.org/10.1063/1.555986.

[15] I. Opticstar, Quotation, 2014.

[16] DMTPC, M. Leyton, J. Phys. Conf. Ser. **718**, 042035 (2016).

[17] J. B. R. Battat *et al.*, Phys. Rept. **662**, 1 (2016), 1610.02396.

[18] D. Dujmic *et al.*, Astropart. Phys. **30**, 58 (2008), 0804.4827.

[19] J. F. Ziegler, M. Ziegler, and J. Biersack, Nuclear Instruments and Methods in Physics Research Section B: Beam Interactions with Materials and Atoms **268**, 1818 (2010), 19th International Conference on Ion Beam Analysis.

[20] R. Veenhof, Nucl. Instrum. Meth. **A419**, 726 (1998).

[21] P. Hamilton, Argon gas measurements in t2k tpc, NuInt UK Workshop, 2015.

[22] Hart, PE, Nilsson, BP, and Raphael, B, IEEE Transactions on Systems Science and Cybernetics SSC4 **4**, 100 (1968).

[23] P. Hamilton, LArIAT: Worlds First Pion-Argon Cross-Section, in *18th International Workshop on Neutrino Factories and Future Neutrino Facilities Search (NuFact16) Quy Nhon, Vietnam, August 21-27, 2016*, 2016, 1611.00821.

[24] P. A. Rodrigues, Tuning generator-based cross-section models, NuFact, 2012.

[25] P. A. Rodrigues, Comparison of mc and theoretical models to recent pion production data, NuInt, 2012.

A Risk Register

Ref.	Risk description	Impact	Likelihood	Mitigation
1.	Loss of key staff from project	Delay to timetable and deliverables	Medium	Ensure good intra-project communication. Enforce good documentation protocol.
2.	Problems with gas system	Delay of pressure vessel and TPC	Low	Design of system using best practice (UK Pressure Equipment Directive) and automated safety systems.
3.	Insufficient TPC gain	Delay of pressure vessel and TPC	Medium	Good communications with TPC experts. Extensive testing before transport.
4.	Damage in transport	Delay of TPC deployment	Medium	Use professional transport company; insurance to protect cost overruns.
5.	Testbeam characteristics different from expectation	Delay in data-taking	Low	Close liasion with CERN.
6.	TOF system performance insufficient	PID performance below expectation; Increase in systematic errors	Medium	Early specification and design of system. System tests before transport to CERN.
7.	Delay or rescheduling of CERN testbeam slot	Delay to project deliverables	Low	Early and frequent contact with CERN testbeam organisers.
8.	Failure of beam during operations	Delay to project deliverables	Low	Close contact with CERN testbeam organisers.
9.	Failure of TPC during operations	Delay to project deliverables	Low	Ensure on-site expert availability.
10.	Failure of ancillary systems during operations	Delay to project deliverables	Low	Ensure on-site staffing by experts; impose data backup and spares availability protocols.
11.	Data loss	Extension to data-taking period; delay in delivery of final results	Low	Impose a data-backup procedure during operation